Atmospheric Pollution Research 5 (2014) 664–676

Atmospheric Pollution Research

www.atmospolres.com

Evaluation of concentrations and source contribution of PM_{10} and SO_2 emitted from industrial complexes in Ulsan, Korea: Interfacing of the WRF–CALPUFF modeling tools

Hyung–Don Lee [1], Jung–Woo Yoo [2], Min–Kyoung Kang [1], Ji–Soon Kang [3], Jong–Hyun Jung [4], Kwang–Joong Oh [1]

[1] *Department of Environmental Engineering, Pusan National University, Busan, 609–735 Korea*
[2] *Division of Earth Environmental System, Pusan National University, Busan, 609–735 Korea*
[3] *Department of Environment Management, Environment Analysis Team, Korea Environment Corporation HQ of Gyeongnam Region, Busan, 616–101 Korea*
[4] *Faculty of Health Science, Daegu Haany University, Gyeongsangbuk–Do, 712–715 Korea*

ABSTRACT

The Ulsan metropolitan city in Korea includes two national industrial complexes [Ulsan Petrochemical Industrial Complex (UPIC) and On–San Industrial Complex (OSIC)] that produce various industrial products. Air pollution from these industrial complexes may pose potential health risks to nearby residential areas. Therefore, WRF–CALPUFF (Weather Research and Forecasting–California PUFF) modeling systems were used to simulate concentration distributions of typical air pollutants (PM_{10} and SO_2), and statistics are computed to determine the models' ability to simulate observations. Finally, we classified the type of business and districts in the region and evaluated their contribution to air pollutant concentrations. Five statistical metrics [Index of Agreement (IOA), Fractional Bias (FB), Normalized Mean Square Error (NMSE), and Pearson correlation coefficient (R)] indicated that the simulated values using CALMET was determined to have sufficient reliability to predict CALPUFF, and simulated concentration field using CALPUFF showed a good agreement [typical values: IOA (0.284 to 0.850 for PM_{10}, 0.412 to 0.895 for SO_2), and FB (0.043 to 0.821 for PM_{10}, –0.393 to 0.638 for SO_2)] with the observed concentrations. The maximum concentrations of PM_{10} and SO_2 using CALPUFF were predicted to be located around OSIC and UPIC, respectively. We compared the simulated values with observed values at 14 monitoring stations, and the SO_2 tended to display better agreement to observed SO_2 values than modeled and observed PM_{10}. The source contribution analysis found that PM_{10} and SO_2 were mostly influenced by group B (35.1%) including steel, machinery, and electronic industry nearby OSIC and group A (40.6%) including chemical industry nearby UPIC, respectively. Finally, the correlations between simulated concentrations of PM_{10} and SO_2 and corresponding emission quantities were 0.663 and 0.528, respectively. Overall, the results of this study could be useful for designing appropriate seasonal regulations to reduce ambient concentrations of air pollutants and assisting environmental administrators to control the sources that contribute the most to degradation of air quality.

Keywords: *Air pollutants (PM_{10}, SO_2), WRF–CALPUFF, source contribution, industrial complex*

doi: 10.5094/APR.2014.076

Corresponding Author:
Kwang–Joong Oh
☎ : *+82-51-510-2417*
🖷 : *+82-51-583-0559*
✉ : *kjoh@pusan.ac.kr*

Article History:
Received: 23 January 2014
Revised: 21 May 2014
Accepted: 21 May 2014

1. Introduction

In the past several years, more and more cities around the globe are experiencing problems from air pollutants emitted from industrial complexes. The environmental damage caused by air pollutants has been simultaneously increasing with the rapidly growing economy and population. In this regard, air pollution episodes have become an important atmospheric phenomenon in cities. Air pollutants can cause serious problems when large–scale industrial complexes are located close to residential areas. In particular, exposure to such air pollutants may adversely affect human health (Ma et al., 2013). Short–term (<1 h) exposure to peak levels of particulate matter has been strongly associated with adverse respiratory health impacts (e.g., respiratory diseases such as asthma and pulmonary function insufficiency) (Hansard et al., 2011). Furthermore, PM_{10} is known to degrade atmospheric visibility. High concentrations of sulfur dioxide (SO_2), which is also emitted from power plants, industrial processes, and during the combustion of fossil fuels, can aggravate respiratory diseases as well as cause problems such as acid rain and damaged vegetation in the form of foliar necrosis (Khamsimak et al., 2012). Therefore, it is necessary to improve methods that can reduce air pollutant emissions from industrial complexes in order to maintain the quality of the atmospheric environment.

Korea ranks 4th in the petrochemicals producing countries around the world, and the city of Ulsan with its rapidly growing industrial developments and economy accounts for 34.9% of the total petrochemical production in Korea. Ulsan encompasses two representative national industrial complexes, namely the Ulsan petrochemical industrial complex (UPIC) and the On–san industrial complex (OSIC). These enormous industrial complexes are confronted with environmental problems stemming from emissions of two typical air pollutants (PM_{10} and SO_2). These air pollutants are regulated by the Korea Ministry of Environment (KME) and other environmental agencies around the world. The U.S. Environmental Protection Agency (EPA) promulgated new National Ambient Air Quality Standards (NAAQS) for fine particulate matter (PM to $PM_{2.5}$) in 1997. The current KME standards for PM_{10} that Korea sets for air quality control are comprised of both a 24–h allowable average and an annual allowable average (a 24–h average of 100 μg/m^3 and annual average of 50 μg/m^3). The standards for SO_2 are comprised of three short– and long–term values [1–h average of 0.15 ppm (~393 μg/m^3), a 24–h average of 0.05 ppm (~131 μg/m^3), and an annual average of 0.02 ppm (~52 μg/m^3)].

SO_2 has been given high priority in research activities in the fields of air pollution and environmental health research in particular (Zou et al., 2011). Importantly, urban air pollution levels of both PM_{10} and SO_2 show frequent temporal and spatial variation (Isakov et al., 2007). Therefore, it is essential to collect many measurements of these air pollutants, which necessitates that local governments maintain the optimized air quality network with a correct spatial distribution according to the specific emissions, orography and weather conditions to determine ambient concentrations as accurately as possible near regional sources.

Specifically, air quality models have proven useful for determining the spatio–temporal distribution of air pollutants and for developing emission control policies that allocate limits to air pollutant emissions (Holmes and Morawska, 2006; Zhang et al., 2010; Ma et al., 2013). Dispersion modeling describes the transport and dispersion of air pollutants, as well as chemical and physical processes within the plume. Such data enable researchers to better analyze air pollutant concentrations in various areas. Many researchers use Gaussian models such as the American Meteorological Society/Environmental Protection Agency Regulatory Model (AERMOD), and the California Puff model (CALPUFF) to evaluate air pollution phenomenon. The CALPUFF model is a multi–layer non–steady state puff dispersion model designed to model the dispersion of particles and gases using space and time varying meteorology (Holmes and Morawska, 2006). This model is also applicable to stagnant conditions (Scire et al., 2000a). In particular, the CALPUFF model has been used to simulate concentration distributions, and health impacts of gaseous and particulate pollutants from various pollution sources and regions (Villasenor et al., 2003a; Lopez et al., 2005; Song et al., 2006; Ghannam and El–Fadel, 2013).

In this study, we calculated the emissions of high priority air pollutants (PM_{10} and SO_2) emitted from national and general industrial complexes, which included point and area sources, in Ulsan, and used the Weather Research and Forecasting (version 3.4 WRF) and CALPUFF models to accurately predict the average meteorological conditions and the concentration distribution (24–h) of PM_{10} and SO_2 during 2012. In addition, we considered the vertical profiles in total domain using the WRF model to complement the few upper data, and analyzed the reliability of the predicted values by comparing them to observed values using statistical techniques. Furthermore, the resulting data were compared to national standard concentrations for PM_{10} and SO_2. Because the industrial complexes in Ulsan are composed of various business types, we evaluated the contribution of different businesses to air pollutant concentrations. The aggregate concentration contribution of pollutants from each source group was assessed using modeling methods. It is hoped that the results from this study will help to improve the air quality in the study area.

2. Methodology

2.1. Topographical and meteorological characteristics of the study area

The metropolitan city of Ulsan is located on the southeastern edge of the Korean Peninsula in a unique strategic location (35°30'–35°43' N and 129°01'–129°36' E) that provides a gateway to the whole Asian continent and the world through its great ports. Ulsan, which represents a typical coastal industrial city in Korea, is surrounded by mountains to the west. The administrative districts of Ulsan are comprised of 5 districts (Buk–gu, Nam–gu, Jong–gu, Dong–gu, and Ulzu–gun), and the area includes two national industrial complexes. In 2012, the total area and population of Ulsan were 1 060 km^2 and 1 153 915 people, respectively. Figure 1 shows a geographic map of the study area and the locations of nearby meteorological stations. In Figure 1, the sky–blue zone shows the extent of the two national and general industrial complexes and the gray zone shows the extent of the residential areas, which includes conventional dwellings, apartments, row houses, and rural structures. The gray line in Figure 1 shows the main road.

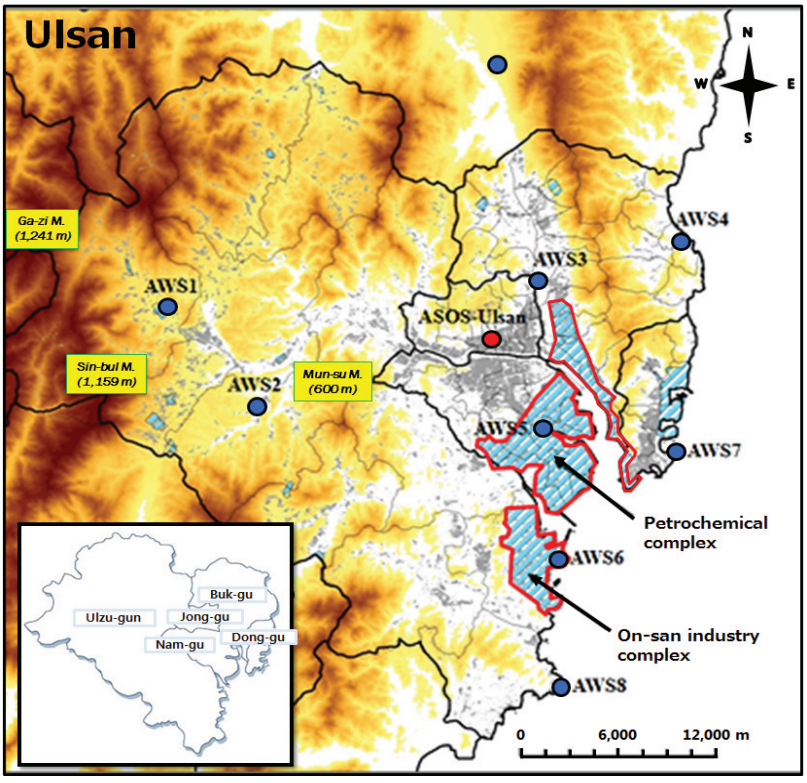

Figure 1. *Location of the two national industrial complexes (diagonal line), topography of the surrounding area in Ulsan, and the location of the nearby meteorological stations (dots).*

Data on meteorological parameters were collected at one Automated Surface Observation System (ASOS) station (red dot) and eight Automatic Weather System (AWS) stations (blue dots) (Figure 1). The meteorological parameters were measured every hour and included temperature, relative humidity, wind conditions, cloud cover, solar radiation, and precipitation. Meteorological data were also obtained from all monitoring stations to analyze the accuracy of the simulated data using CALMET as compared to observational data.

Table S1 shows the meteorological conditions in Ulsan (see the Supporting Material, SM). The lowest and highest average temperatures are –11.6 °C in winter and 35.4 °C in summer, and annual mean temperature and humidity is 13.7 °C and 63% (maximum value: 74.7% in summer, and minimum values: 52.3% in winter). Total annual precipitation is ~1 458.1 mm (spring: 298.8, summer: 517.8, autumn: 499.1, winter: 149.1 mm). The average of sunshine hours is 190.7 h, and clear days in summer are rare in comparison with other seasons due to frequent precipitation. The average wind direction mostly consisted of northwesterly winds (N, WNW, NW, and NNW), and the average wind speed was usually lower than 3.0 m/s (2.1–2.8 m/s) in all seasons. The annual prevailing wind direction for Ulsan was N and WNW during all seasons because Korea is generally influenced by the westerly winds blowing across the peninsula. In particular, the dispersion of air pollutants can be affected greatly by wind direction patterns, thus it is important to understand the meteorological conditions present in industrial and residential areas. In other words, studies on the concentration distribution and dispersion of air pollutants must analyze meteorological data in an area as wide as possible, in accordance with available data from all measurement stations.

2.2. Real–time air quality system for pollutants

In this study, we used data observed from real–time monitoring system installed in each station to measure PM_{10} and SO_2. The instrumentations for PM_{10} and SO_2 were BAM–1020 (Met One, USA) and 100E (API, USA), respectively, and were installed on top of the buildings in the major area. Table S2 (see the, SM) shows the overall specifications and measuring method.

2.3. Model description and evaluation approach

The CALPUFF is a non–steady–state, multi–layer Lagrangian puff model for the estimation of deposition/concentration patterns for multiple air pollutants by considering the effects of space–time varying meteorological conditions. Puff dispersion is Gaussian, and concentrations are based on the contribution of each puff as it passes over or near a receptor point (Zhou et al., 2003). The CALPUFF model was adopted following recommendations from the U.S. EPA for its use in modeling the dispersion of air pollutants from various sources in industrial complexes (Scire et al., 2000a; Ghannam and El–Fadel, 2013). The CALMET model used for generating meteorological input data for the CALPUFF model, calculates hourly wind and temperature fields on a three–dimensional (3D) gridded modeling domain. In addition, it produces mixing height, surface characteristics, and dispersion properties (Tartakovsky et al., 2013). Emission quantities and CALMET outputs are the input data into the CALPUFF model. Finally, the CALPOST program is a postprocessor for results from CALPUFF simulations.

In this study, meteorological data over an annual period of 1 year (2012), which were collected from 9 surface stations, were input into CALMET to generate the diagnostic meteorological field. The innermost domain (D3) of the WRF model and 14 air quality monitoring sites are shown in Figure S1 (see the SM). The gridded geophysical data including land use and terrain height were generated from the U.S. Geological Survey (USGS) terrain and land use database. The basic horizontal grid–cells (1 km x 1 km) for CALMET consisted of 90 grid cells along the x–axis and 90 grid cells along the y–axis (90 km x 90 km) and the domain, specified at the southwest corner, spanned 3 900.5 km north and 470.5 km east in UTM zone 52. In the vertical dimension, the 8 vertical layers incorporated into CALMET modeling had heights of 20, 50, 100, 200, 500, 1 000, 1 500, and 2 000 m.

In this study, we used the prognostic meteorological model WRF to provide dynamic meteorological fields for the CALMET model in the CALPUFF model system. The WRF model description including physical process was detailed in Table S3 (see the SM). The WRF was initialized with the single–moment 6–class scheme, Kain–Fritsch scheme, and the Yonsei University PBL parameterization was used to represent the PBL over the domain (Hong et al., 2006; Mohan and Bhati, 2011). Rapid radiative transfer model (RRTM) scheme was applied and the Noah Land Surface model was used to calculate the heat and moisture content of each sub–soil layers (Liu et al., 2013).

The 3D analysis fields obtained from the Final Operational Global Analysis (FNL) from the National Center for Environmental Prediction (NCEP) were used to provide initial and boundary conditions for WRF simulations. The NCEP FNL fields were at 6 h intervals with a spatial resolution of 1° (Abdul–Wahab et al., 2011; Liu et al., 2013). The WRF simulations were performed for three nested domains with grid resolutions of 27 km, 9 km, and 3 km. The final nested domain (D3) had horizontal 49 x 52 grid cells, and 28 vertical layers were used. The interface program (CALWRF) has been developed which processes the output from WRF to be used as the initial guess for meteorological field of CALMET (Scire et al. 2000b). In this study, the data in WRF output files were interpreted and converted to a format compatible with CALMET by CALWRF program.

In dispersion options for CALPUFF, we applied the dry deposition and wet removal options assuming they behave as particles to incorporate the precipitation data from the observing stations. The mean and standard deviation are used to compute a deposition velocity for a size–range, and these are then averaged to obtain a mean deposition velocity, and we used the size distribution for PM_{10} (5 μm). For wet deposition, scavenging coefficients for liquid precipitations were set at $1x10^{-4}$, and $3x10^{-5}$ for PM_{10}, and SO_2 (Zhou et al., 2003; Hao et al., 2007). The miscellaneous dry deposition parameters included the reference cuticle (30 s/cm), and ground (10 s/cm) (Villasenor et al., 2003a), and the chemical transformations (MESOPUFF II scheme) were computed internally. This chemical transformation is the conversion of SO_2 to sulfate and the conversion of nitrogen oxides to nitrate aerosol and these reactions included the gas phase and photochemical reactions with background pollutants (e.g. O_3 and NH_3) (Scire et al., 2000a). But the chemical reaction option such as background concentrations (precursor gases: NH_3, H_2O_2, NO, NO_2, and secondary organic aerosol) was not considered in this study, and all the emission sources were considered to be point and area sources.

2.4. Statistical evaluation of model performance

The most commonly used measures of model performance are the statistics recommended in the U.S. EPA 1992 modeling guidance. To determine the reliability of the simulation data, verification of simulated values using the WRF model was conducted for surface temperatures and wind data at monitoring sites over one year using several statistical indicators (Song et al., 2006; Cai and Xie, 2010; Gupta and Mohan, 2013). In particular, the statistical verification of model performance in this study was performed using five statistical indicators including the Index of Agreement (IOA), Fractional Bias (FB), Normalized Mean Square Error (NMSE), and Pearson correlation coefficient (R). The formulas used to derive these five indicators are given in Equations (1)–(5):

$$IOA = 1 - \frac{\sum(P_i - \bar{O}_i)^2}{\sum(|P_i - P_i| + |O_i - \bar{O}_i|)^2} \quad (1)$$

$$FB = \frac{(\bar{O}_i - \bar{P}_i)}{0.5(\bar{O}_i - \bar{P}_i)} \quad (2)$$

$$NMSE = \frac{\overline{(\bar{O}_i - \bar{P}_i)^2}}{\overline{O_i P_i}} \quad (3)$$

$$RMSE = \sqrt{\frac{1}{N}\sum_{i=1}^{N}(P_i - O_i)^2} \quad (4)$$

$$R = \frac{\left(\overline{O_i - \bar{O}_i} - \overline{P_i - \bar{P}_i}\right)}{\sigma P_i \sigma O_i} \quad (5)$$

where, N represents the number of data, P_i and O_i are the predicted and observed concentrations, respectively, and $\bar{P}_i$ and $\bar{O}_i$ are the mean values of the predicted and observed concentrations, respectively. Likewise, σP_i and σO_i are the standard deviations of the predictions and observations.

The IOA varies from 0.0 (i.e., theoretical minimum value for an inaccurate prediction) to 1.0 (i.e., perfect accuracy between the predicted and observed values), and IOA values above 0.5 are considered to represent good predictions (Zawar–Reza et al., 2005). Therefore, Equation (1) reflects the degree to which the observed variable is accurately assessed by the simulated values (Willmott, 1984; Levy et al., 2009). The FB is normalized to make it dimensionless, and values can vary between +2 and –2; values of zero represent an ideal model and negative and positive FB values represent over–predictions and under–predictions, respectively (Chang and Hanna, 2004). The NMSE emphasizes the scatter in the entire data set, and smaller values of NMSE denote better model performance. The RMSE value should be close to zero for good accuracy.

3. Results and Discussion

3.1. Analysis of emission source inventory

Table S4 (see the SM) shows the overall emission inventory of area and point sources and the contribution of each source category to SO_2 and PM_{10} concentrations in the administrative district of Ulsan. Stack characteristics of point sources are also listed in Table S5 (see the SM). For this study, the emission quantities emitted from point sources were obtained from a Tele–Monitoring System (TMS) installed at chimneys at each factory in Ulsan for one year. For annual emission of area sources, we used the Clean Air Policy Support System (CAPSS) provided by the Environmental Management Division in Ulsan. To accurately and realistically estimate the administrative district level air pollutant emissions of Korea, the CAPSS data was developed, and total emissions from area sources were basically estimated by the multiplication of emission factors and relevant activity data in consideration of the removal efficiencies of control devices (Lee et al., 2011).

Total PM_{10} emissions were estimated to be 6 667.6 tons/yr, with point sources accounting for approximately 96.8% (6 455.7 tons/yr) of the total. This latter estimate includes OSIC emissions of around 45.1% (3 003.5 tons/yr) and emissions from point sources in the UPIC of 40% (2 666.8 tons/yr). The total contribution of area sources was very low (approximately 3.2%). In contrast, total SO_2 emissions (63 877 tons/yr) were approximately 10 times higher than PM_{10} emissions, because the most plants in Ulsan used the high–sulfur fuels such as coal and bunker fuel for a long time. The SO_2 emissions emitted from point sources in the UPIC in Nam–gu were the highest at 35 942.5 tons/yr (56.27%). Other SO_2 emissions for point sources were lower and these included emissions from Ulzu-gun (43.19%), and Buk-gu (0.36%). On the other hand, total area sources for SO_2 emissions only were 0.36 %.

3.2. Evaluation of meteorological simulations

To investigate the reliability of the meteorological simulation results, four statistical verification indices (IOA, FB, NMSE, and RMSE) were used to compare the modeled and observed data from typical meteorological monitoring sites. Table S6 and S7 (see the SM) show the statistical evaluation results for WRF and CALMET (AWS observation + WRF) for temperature and wind speed. In the meteorological assessment of WRF modeling, the IOA values were 0.9429 (0.9180 to 0.9579) for temperature, and 0.5511 (0.4782 to 0.6764) for wind speed. The average of FB, NMSE, and RMSE values were 0.0283, 0.0030, 4.6433 for temperature, and –0.6536, 1.2619, 4.0684 for wind speed, respectively. In the meteorological assessment of CALMET modeling, the highest estimated IOA values were 0.9986 (0.9972 to 0.9998) for temperature, and 0.9624 (0.9174 to 0.9867) for wind speed. The FB values for all stations were encouragingly very low than WRF results, and they ranged from –0.0021 to 0.0031 for temperature, and 0.0063 to 0.4158 for wind speed. The NMSE and RMSE values were also very low than WRF results, and average values were found to be 0.0026 and 0.6848 for temperature, and 0.0723 and 0.5906 for wind speed, respectively. Overall overestimation using WRF was improved as compared with observation data. From these results, the quantitative evaluation of the simulation revealed that the CALMET model performance was better for meteorological factors in comparison to WRF model. Consequentially, these results indicated that the CALMET simulation for surface data and WRF for vertical profile must be conducted to analyze accurately the concentration and dispersion of pollutants. Therefore, the meteorological simulation was determined to have sufficient reliability and precision to predict the dispersion and concentration distribution of PM_{10} and SO_2 using the CALPUFF.

Figure 2 shows the wind roses that were constructed from simulated data using the CALMET model and observed annual average data at major stations (one inland area and four coastal areas). Overall, the simulated results corresponded well with the observed ones. The wind field distribution at the AWS 2 station, which is located in an inland area near the mountains, was dominated by southwesterly and east winds. However, northwesterly, north, and northeasterly winds were mostly predominant at the AWS stations located nearby coastal areas, and these winds can affect the diffusion of air pollutants emitted from UPIC and OSIC. The wind direction at the AWS 4 station was predominantly westerly, which was exceptional for the coastal stations. This was caused by geographical and topographical effects such as those from mountains located in the northwest and southwest directions.

The average wind speeds nearby the coast were stronger than those in inland areas, and the proportion of calm winds (<0.5 m/s) was only 0.1–1.98% in the coastal area. In contrast, calm conditions were often present in the inland area (34.96–41.21%). Wind speed in the coastal area was influenced by local winds such as land–sea breezes, and cyclical patterns of the land–sea breezes may play a significant role in determining air pollutant dispersion and transport in industrial regions near the coastal areas (Levy et al., 2009). Hence, wind direction patterns in the study area were monitored consistently, and this should be continued in future research.

3.3. Concentration distribution of air pollutants

The seasonal average concentration distributions of PM_{10} and SO_2 in Ulsan are plotted in Figure 3. The seasonal values were determined from data collected during four months (January, April,

July, and October) in 2012, and the simulated results are given as 24–h intervals. The seasonal patterns of PM_{10} and SO_2 concentrations were shifted from source areas in the southeast direction during autumn and winter, while the patterns in the spring and summer were diffused in the northeast and west directions. High concentration events in residential areas are more likely to occur during the summer. Consequently, the dispersion of air pollutants in this study was mainly dependent on the meteorological conditions (i.e., various types of wind distribution and strength), and this finding has also been observed by others (Choi and Fernando, 2007).

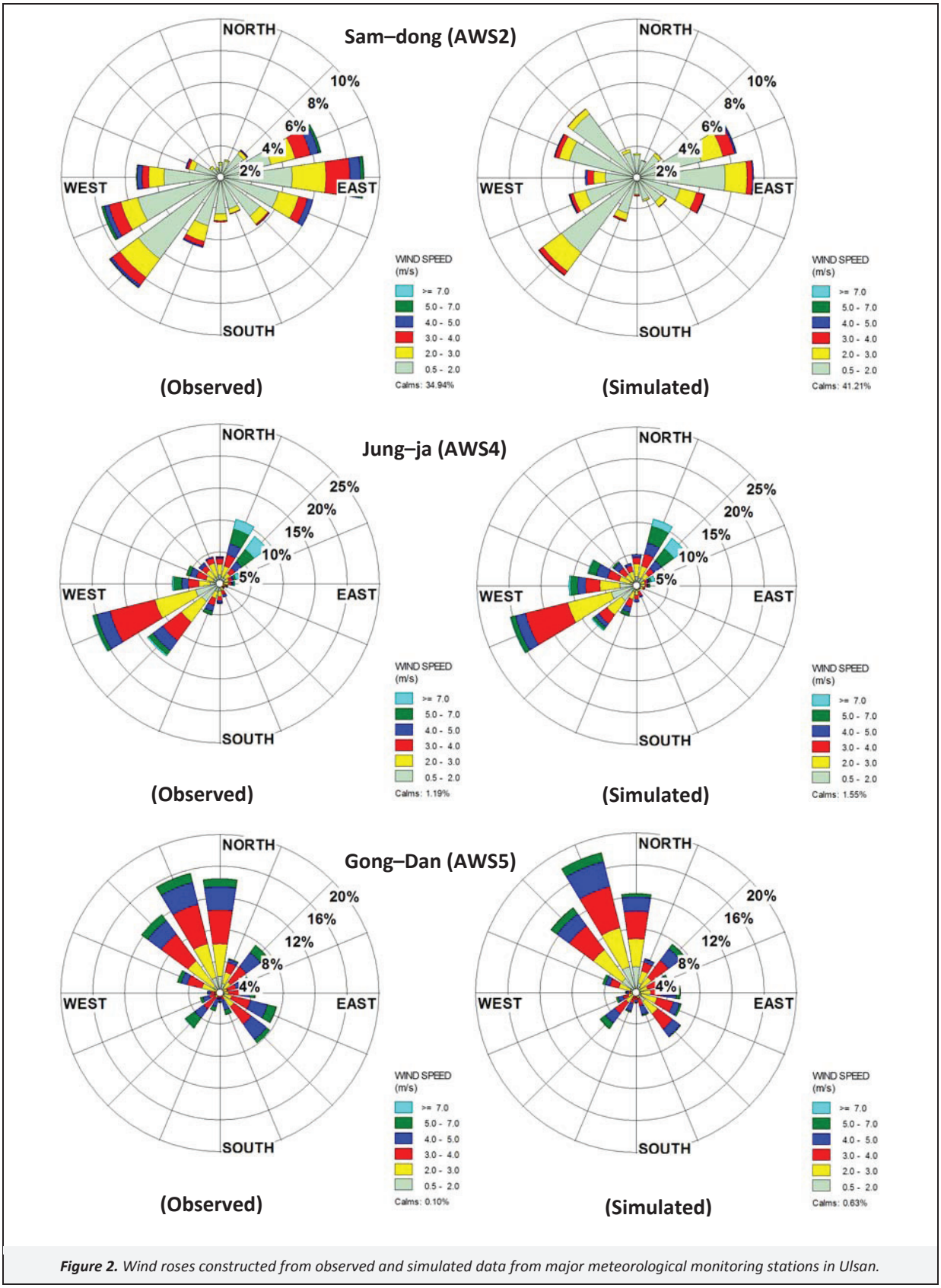

Figure 2. *Wind roses constructed from observed and simulated data from major meteorological monitoring stations in Ulsan.*

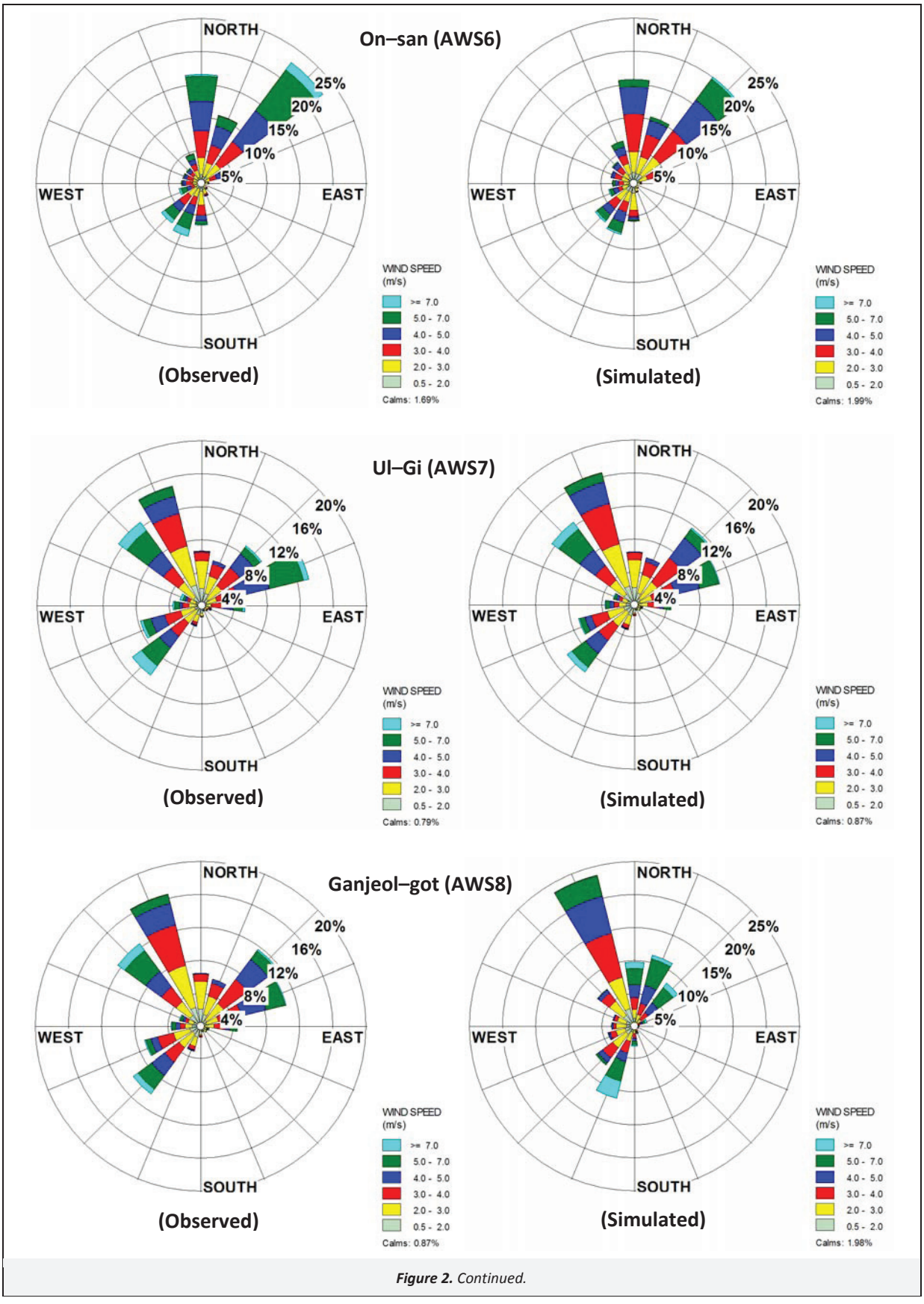

Figure 2. *Continued.*

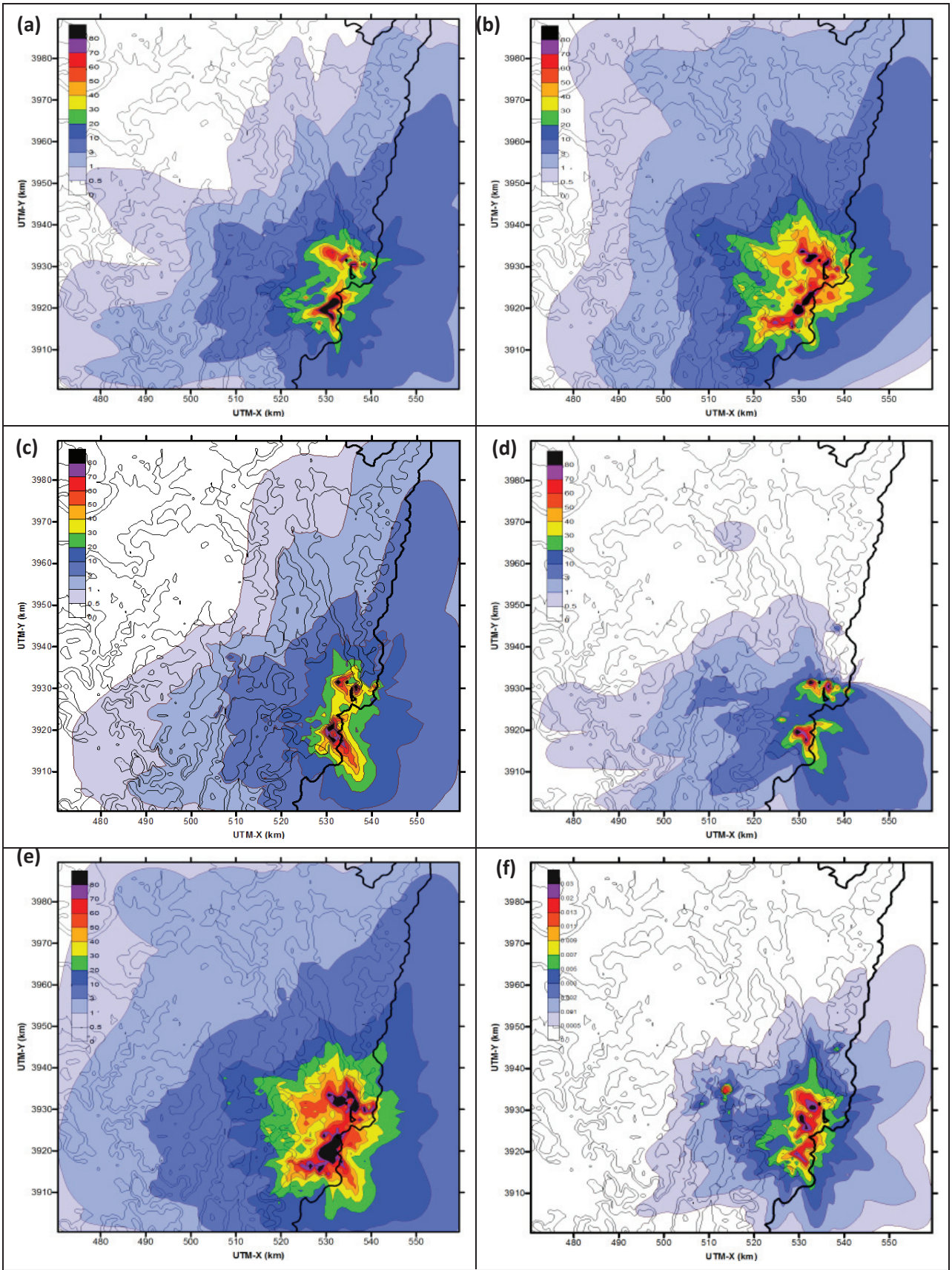

Figure 3. *Predicted surface PM_{10} concentration ($\mu g/m^3$) field during* ***(a)*** *spring (4.1),* ***(b)*** *summer (7.1),* ***(c)*** *autumn (10.30),* ***(d)*** *winter (1.1), and* ***(e)*** *the annual (1.1); SO_2 concentration (ppm)* ***(f)*** *spring (4.30)*

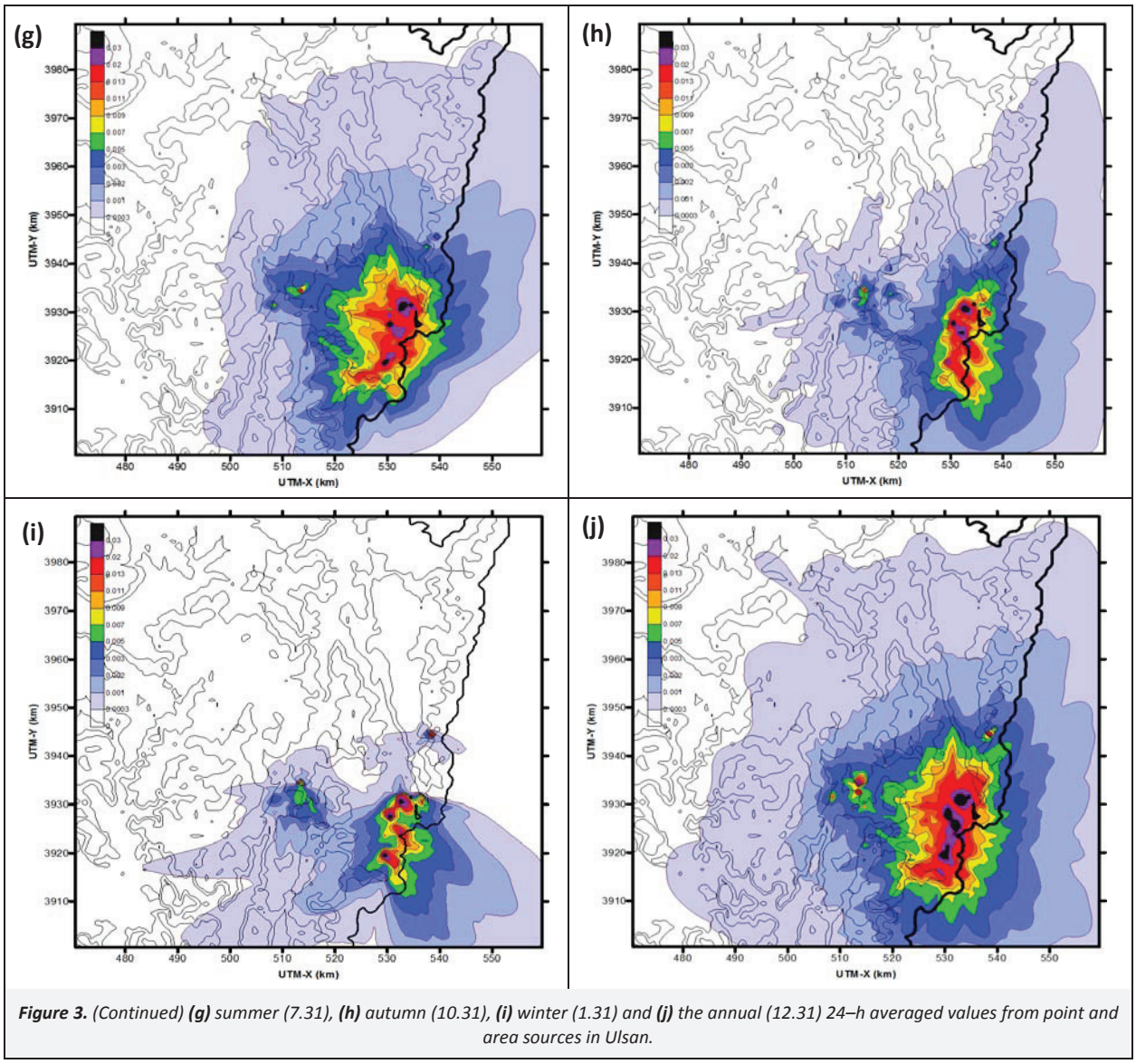

Figure 3. *(Continued)* ***(g)*** *summer (7.31),* ***(h)*** *autumn (10.31),* ***(i)*** *winter (1.31) and* ***(j)*** *the annual (12.31) 24–h averaged values from point and area sources in Ulsan.*

The PM_{10} and SO_2 average concentrations in most regions were below 24–h environmental criteria of 100 μg/m^3 and 0.05 ppm, respectively. The plumes of PM_{10} emissions from sources dispersed effectively in all directions during the simulation period except for during winter where the radius of impact was approximately 50 km. The maximum 24–h averaged PM_{10} concentrations during the simulation period ranged from 0.34 to 157.7 μg/m^3 in spring, 0.21 to 134.3 μg/m^3 in summer, 0.24 to 115.9 μg/m^3 in autumn, and 0.17 to 111.8 μg/m^3 in winter, and average concentrations generally were below the standards. Peak concentrations were frequently predicted in the same areas, and high accumulation levels were obvious during the spring time where there were extensive zones of influence near emission sources (OSIC and UPIC). The PM_{10} emitted from the sources accounted for more than 95% of the entire emission amount (see the SM, Table S4). Hence, the distributions of the simulated maximum PM_{10} concentrations by CALPUFF were able to clearly identify nearby sources.

Similarly, the annual maximum concentrations for SO_2 were found around the sources. Similarly, the annual maximum concentrations for SO_2 were found around the sources, and the dispersion distribution for 2012 indicates that there was a radius of impact of approximately 40 km around the sources. The simulated concentrations of SO_2 averaged for the seasonal periods of spring, summer, autumn, and winter at monitoring stations were 0.0135, 0.0132, 0.0112, and 0.0088 ppm, respectively. Notably, the concentrations during the summer negatively affected nearby residential areas due to exacerbating meteorological conditions such as wind direction (SE) and high average wind speeds. Generally, the variation of mixing height were found to be higher in winter than in summer (Rama Krishna et al, 2004), and the atmospheric boundary layer (ABL) heights were particularly low in summer since high precipitation interrupted the increasing of ABL height. Hence the specific seasonal change hampered far dispersion of pollutants in summer, but this phenomenon does not continue for a long time by precipitation. Specifically, high wind speeds and increased turbulence in the coastal area can transport air pollutants further downwind from the source areas (Kesarkar et al., 2007). In addition, the sea breezes, which are generated by differences of specific heat between the land and sea in the coastal area, occur frequently during the summer. This is because solar radiation energy is stronger in the summer than in other seasons. Therefore, the modeling results were influenced by the wind patterns (northeasterly and southeasterly), which were associated with sea breezes. In consideration of these findings, air quality regulations and monitoring programs should be designed so that seasonal and temporal variations in air pollutant concentrations caused by weather conditions are taken into account.

3.4. Evaluation of CALPUFF modeling performance

We obtained the valid values from hourly data (e.g. over nine values of 5 minutes during 1 hour are valid), so quality criterion is over 75%. The PM_{10} and SO_2 concentrations observed at the 14 ambient monitoring stations were compared to the CALPUFF simulated values (Figure 4). From Figure 4, it can be seen that values predicted using the CALPUFF were below the observed values. Because the background concentrations were not included in CALPUFF simulation results (i.e., regional baseline pollutant levels and/or uncertain emissions) or account for air pollutants that may have been transported into the study area from line sources and sources outside the study area. Thus, the modeling method used here would not be advisable to use for predicting quantitative concentrations in the strict sense (Kesarkar et al., 2007). Nevertheless, many researchers have used this type of modeling method to evaluate air quality in target areas (Villasenor et al., 2003b; Song et al., 2006; Zou et al., 2011; Ghannam and El–Fadel, 2013; Ma et al., 2013; Tartakovsky et al., 2013), and it is generally assumed that uncertain emissions and background concentrations are constant factors during the research period.

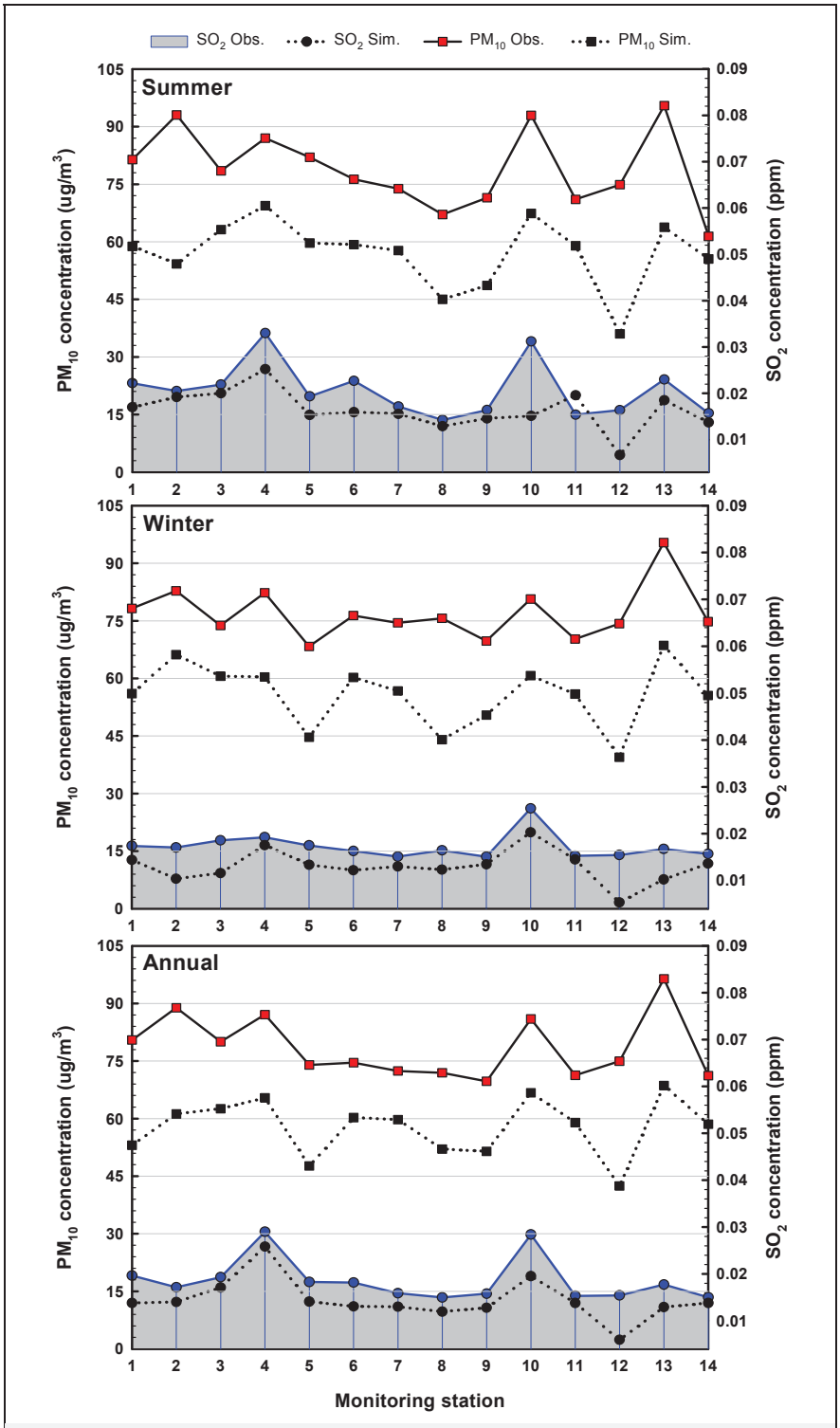

Figure 4. *Comparison of 24–h simulations with observed data for PM_{10} and SO_2 at 14 monitoring sites during various seasons (summer, winter, and annual values).*

The simulated values for SO_2 were similar to the observed concentrations, and overall, the concentration distributions for SO_2 were relatively more analogous to the observed values than the PM_{10} concentration distributions. These results could not represent air quality and have some limitations, because secondary pollutant ($PM_{2.5}$, and secondary organic aerosol) formation was not included in this study. However, the Korean government regulated only the as particle matter (as PM_{10}), so it is also important to note the overall concentration distribution and level of contribution for PM_{10} to control air quality problems in industrial complex area. This was likely because sources of particulate matter including PM_{10} can be generated by human activities (i.e., fuel combustion from power plants, burning of fossil fuels by vehicles, and various industrial processes) as well as by natural processes (i.e., forest fires and volcanoes). Especially, PM_{10} can affect neighboring countries for thousands of kilometers during intercontinental transport such as those caused by Asian dust events, affecting much of East Asia sporadically during spring (Gupta and Mohan, 2013). The error of measured concentrations can be occurred by vapor and sea salt by sea breeze in Ulsan, located in seaside. As a result, PM_{10} is more influenced by other sources than SO_2. Hence, PM_{10} concentrations simulated using CALPUFF may be generally limited to producing accurate predictions in specific topographic areas. In contrast, SO_2 is largely generated during the combustion of fossil fuels such as coal and petroleum that contain high amounts of sulfur, and the major SO_2 sources include power plants, industrial processes, heating equipment, metal smelting, and oil refineries. Therefore, the concentration distributions for SO_2 found in this study were more accurate than PM_{10} concentrations because the SO_2 concentrations were mainly influenced by the modeling input data, which were the emissions of sources in Ulsan (see the SM, Table S4).

Despite the differences in the simulated and observed data discussed above, the concentration distributions of PM_{10} and SO_2 were largely affected by point and area sources in the region. Therefore, if we can evaluate the major sources and determine their relative contributions to air quality degradation in Ulsan, it may be possible to implement air pollution reduction policies that can substantially improve air quality. Table S8 (see the SM) shows a summary of the statistical analysis whereby CALPUFF simulations were correlated to observations for each pollutant spatially (district) based on seasonal average concentrations and temporally (season) during the modeling period summarized all the districts. The *R* values for the correlations between simulated and observed PM_{10} and SO_2 concentrations at all sites were generally high, with the exception of Jong–gu (0.412 for PM_{10} and 0.577 for SO_2), and the location that exhibited the highest *R* valuee was Ulzu–gun (0.806 for PM_{10} and 0.914 for SO_2). In addition, the *R* values from spring to winter, and annual periods were found to be 0.377, 0.598, 0.554, 0.567, and 0.596, for PM_{10}, and 0.558, 0.837, 0.575, 0.764, and 0.768 for SO_2, respectively. The IOA values were generally high and ranged from 0.503 to 0.850 for PM_{10} and 0.657 to 0.895 for SO_2. Recall that the perfect value for IOA is 1 (Gibson et al., 2013); hence, these results are not perfect, but they do represent reasonable predictions. Values for FB and NMSE ranged from 0.043 to 0.821 and 0.014 to 5.502, respectively, for PM_{10}, and –0.393 to 0.638 and 0.023 to 2.750 for SO_2, respectively. Thus, the FB values except autumn were positive indicating that there is under–prediction by the CALPUFF model (Gupta and Mohan, 2013). FB values for reasonable predictions are generally around ±0.15 to ±0.30 (Spak and Holloway, 2009) Hence, these values indicated that the model agreed with the observed concentrations to an acceptable degree.

The RMSE values for PM_{10} and SO_2 ranged between 3.960 and 18.093 and between 0.601 and 6.099, respectively. Furthermore, temporal (seasonal) fluctuation was not as close to the values for spatial classifications (location), but generally we obtained satisfactory results. Overall, the simulated concentration field produced using statistical techniques showed a good agreement with the observed concentrations.

3.5. Analysis of source contribution

The analysis of the relative contributions from different activities to air quality is very important because such data are necessary to determine the types of sources that are most effective on average air pollutant concentrations in industrial complexes. In this study, the sources were categorized according to four subgroups (see the SM, Table S9) in Ulsan. We evaluated the contributions for these groups using CALPUFF concentrations that were generated under the same emission and meteorological conditions to identify problematic sources during 2012. The 24–h average concentration distributions for PM_{10} and SO_2 for the four subgroups (A–D) are shown in Figure S2 (see the SM). Figure 5 shows the converted percentages for the concentration contributions, and the data are presented for monitoring stations.

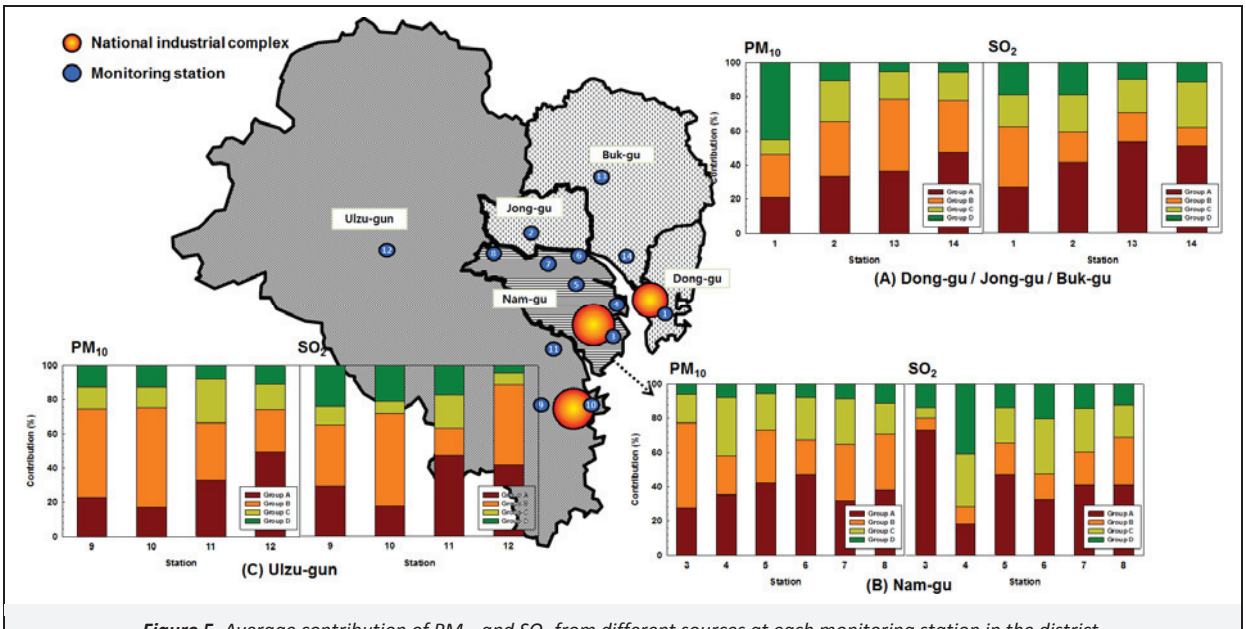

Figure 5. *Average contribution of PM_{10} and SO_2 from different sources at each monitoring station in the district.*

For Group A, total PM_{10} and SO_2 contributions were in the range of 16.9% to 49.2%, and 17.5% to 73.3%, respectively. Importantly, SO_2 pollution from the OSIC could have adverse effects on southern regions because of the prevailing wind direction, which includes northwesterly and northerly winds. Even though the station 11 was located in the center of the UPIC and OSIC, its SO_2 contribution level (47.5%) was likely influenced by emissions from Group A. This was because the wind direction was mainly northwesterly and northerly at AWS 5 and 6 (Figure 2). For Group B, the total PM_{10} and SO_2 contributions ranged from 20.3% to 58.7%, and 6.8% to 54.6%, respectively. The contribution was highest at station 10 because of the high plant density and emissions in the UPIC. The lowest contribution was in the range of 6.8–27.9% for SO_2 in Nam–gu; this is because the chemical industry in Group A relatively had a dominant and widespread influence in this area. In addition, the pollutants by the UPIC could not influence Nam–gu strongly because these pollutants were readily blown to southern–western areas by predominant northerly winds at AWS 6 (Figure 2).

In case of Group C, the contributions for PM_{10} and SO_2 ranged from 8.7% to 34.1%, and 7.0% to 32.6%, respectively (Figure 5). The average contribution levels from Group C were generally lower than group A. For Group D, the contributions for PM_{10} and SO_2 ranged from 4.9% to 45.1%, and 4.3% to 41.1%, respectively. While station 4 located near the UPIC mostly belongs to Group A, the data indicate that SO_2 emitted from Group D strongly influenced the overall contributions in this area. This is probably because this area is located in the center of the modeling target area, and influenced by northwesterly and northeasterly winds at AWS 7. In addition, the stack heights of the sources in Group D tended to be very short except for a few ones. Consequently, even though the emissions were small, the dispersion of pollutants away from sources was likely low; therefore, the contributions were more widespread and high throughout Ulsan (Song et al., 2006). Finally, we suggest that unnecessary monitoring stations must be removed to reduce operating expenses, and number of optimum station was 10, except several stations (5, 6, 7, 14) concentrated in the district.

Table 1 shows the contributions of PM_{10} and SO_2 classified by district. In the case of Group A and B for PM_{10}, the contributions showed similar tendencies to those of emissions.

The emission contribution for Group A had a similar value to the average, also the emission contribution for group B was and similar to the average for PM_{10}. The average contributions of group C and D increased from 14.6 to 19.6%, and 5.9 to 11.0%, respectively. But, in the case of group A for SO_2, the emission contribution (67.3%) was different from the average contribution (40.6%), and in case of Groups B, C, and D, average contributions (22.7%, 19.8%, and 16.8%, respectively) increased in comparison with the emission contributions in proportion to the reduced contribution rate of Group A. This means that ambient concentrations were influenced by the stack heights of the sources and meteorological parameters. The stack heights at OSIC were on average lower than the heights at UPIC (see the SM, Table S5). Specifically, the air pollutants are subject to atmospheric dilution when the wind speed is high. Consequently, ground level pollutant concentrations in downstream areas from emission sources will be low.

3.6. Analysis of correlation

We performed a correlation analysis between simulated concentrations obtained from the CALPUFF model and PM_{10} and SO_2 emissions. The data were analyzed on a logarithmic scale, and the results are shown in Figure 6. The coefficient of determination (r^2) for PM_{10} and SO_2 was 0.663 and 0.528, respectively. Overall, the coefficient of determinations obtained for Ulsan showed moderately high correlations, and the PM_{10} value was higher than the SO_2 values in particular. Consequently, high emission quantities (i.e., SO_2) do not necessarily mean that ambient air concentrations will also be high, but there is a general tendency for this to occur. In addition to emission quantities, the concentrations of air pollutants in Ulsan were influenced by the stack heights and by meteorological conditions. Therefore, industrial plants should consider adjusting stack heights and outlet velocities to reduce the ambient air concentrations of pollutants at vulnerable receptors located near the plants. In the future, we would like to conduct additional evaluations regarding diurnal variations, such as those that may occur during the daytime and nighttime, in order to ascertain source contributions and devise more specific solutions that may lead to reduced environmental and health risks.

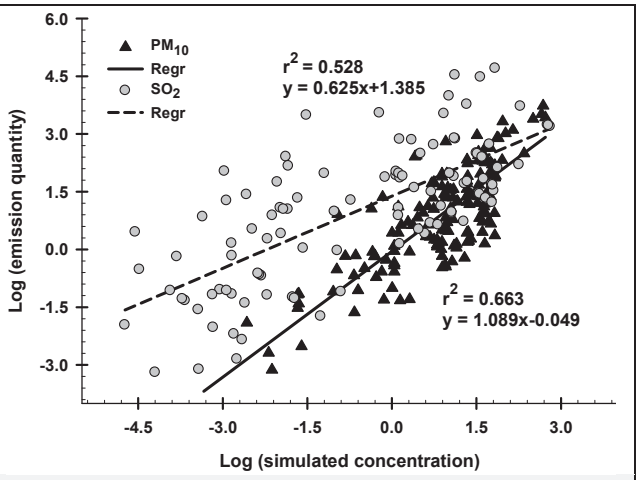

Figure 6. *Correlations between simulated concentrations and emissions.*

4. Conclusion and Limitations

In this study, the WRF/CALPUFF couple modeling system was employed to simulate PM_{10} and SO_2 dispersion distribution data for emissions from multi–stack industrial sources in Ulsan. We evaluated the source contributions as categorized by source types to better understand what is driving air pollutant concentrations in the region, and the results may enable environmental administrators to implement more effective emission reduction policies in Ulsan. Modeling evaluations showed that there were spatial variations in regional air quality conditions. Thus the data were more useful for understanding the ambient air concentration distributions in the target area than observational data, which is collected from sparsely located air quality monitoring sites.

Four statistical indicators were used to verify the reliability of the WRF simulation results, and the simulated data generally showed good agreement with the observed data. The results for the dispersion distribution of two air pollutants, PM_{10} and SO_2, showed that fluctuations in the spatial distribution were associated with seasonal meteorological conditions such as wind speed, direction, and local winds (sea breezes). Maximum concentrations were observed during the spring and summer seasons, therefore environmental administrators and managers should target regulatory actions to these worst case scenarios. Finally, we analyzed the level of contribution from different source types and districts, and conducted correlation analyses between emissions and predicted air concentrations. The regional PM_{10} and SO_2 concentrations were predominantly associated with group B (35.1%) nearby the OSIC area and group A (40.6%) sources nearby the UPIC area, respectively. In addition, moderately high correlations (0.663 for PM_{10}, 0.528 for SO_2) were found between the source emissions and simulated concentrations. However, the data indicated that large emissions did not always correspond to high concentrations in the areas surrounding the sources. Stack heights and exit velocities were identified as important factors that may affect pollutant dispersion and atmospheric concentrations in the region. We hope that the results of this study will be used to prioritize emission control and mitigation efforts and improve the overall air quality.

Table 1. *The contributions of PM_{10} and SO_2 in the district*

	Group	Emission (%)	Contribution (%) by District					Average (%)
			(A) Dong–gu+Jong–gu+Buk–gu	(B) Nam–gu	(C) Ulzu–gun	Industry	Resident	
PM_{10}	A	38.3	32.1	37.1	30.4	25.2	37.6	34.3
	B	41.2	31.1	31.5	42.4	39.0	33.6	35.1
	C	14.6	16.5	23.7	16.3	18.0	20.2	19.6
	D	5.9	20.3	7.8	10.9	17.8	8.5	11.0
SO_2	A	67.3	40.4	42.2	34.0	34.0	43.0	40.6
	B	18.3	22.4	14.8	38.3	24.8	22.0	22.7
	C	5.5	21.2	23.9	11.2	17.7	20.6	19.8
	D	8.9	16.0	19.1	16.6	23.6	14.3	16.8

This research had the several limitations. First, we assumed that each source consistently emitted air pollutants during the simulating period, and we were not able to account for background concentrations of modeled and other pollutants (e.g., NH_3) and air pollutants transported from line sources outside of the study area. Hence, it was difficult to accurately predict concentration trends using the CALPUFF model and simulated data routinely under–estimated the observed values. Nevertheless, the simulated data were valuable for visualizing the overall dispersion distribution for PM_{10} and SO_2 and for identifying the primary contributors to air quality problems.

Acknowledgments

This work was supported by the Brain Korea 21 Plus Project in the Division of Creative Low Impact Development and Management for Ocean Port City Infrastructures.

Supporting Material Available

Average meteorological characteristics for Ulsan in 2012 (Table S1); Characteristics of the measuring equipment for PM_{10} and SO_2 (Table S2); The WRF simulation option (Table S3); Air pollutant emissions and contributions from point and area sources located in the industrial complexes of Ulsan (Table S4); Stack characteristics from point sources at the industrial complexes (Table S5); Statistical verification for the WRF simulation at meteorological monitoring sites (Table S6); Statistical verification for the CALMET simulation at meteorological monitoring sites (Table S7); Statistical analysis of model simulations at the district (Table S8); Characteristics of major source groups in Ulsan (Table S9); Simulation domains for (a) the nested domain configuration of the WRF model and (b) detailed topography of the final nesting domain (D3) located at 12 surface stations and 14 air quality monitoring sites (Figure S1); and PM_{10} and SO_2 concentration contributions (24–h) from each group for 2012 (Figure S2). This information is available free of charge via the Internet at http://www.atmospolres.com.

References

Abdul–Wahab, S., Sappurd, A., Al–Damkhi, A., 2011. Application of California Puff (CALPUFF) model: A case study for Oman. *Clean Technologies and Environmental Policy* 13, 177–189.

Cai, H., Xie, S.D., 2010. A modelling study of air quality impact of odd–even day traffic restriction scheme before, during and after the 2008 Beijing Olympic Games. *Atmospheric Chemistry and Physics* 10, 5135–5184.

Chang, J.C., Hanna, S.R., 2004. Air quality model performance evaluation. *Meteorology and Atmospheric Physics* 87, 167–196.

Choi, Y.J., Fernando, H.J., 2007. Simulation of smoke plumes from agricultural burns: Application to the San Luis/Rio Colorado airshed along the U.S./Mexico border. *Science of the Total Environment* 388, 270–289.

Ghannam, K., El–Fadel, M., 2013. Emissions characterization and regulatory compliance at an industrial complex: An integrated MM5/CALPUFF approach. *Atmospheric Environment* 69, 156–169.

Gibson, M.D., Kundu, S., Satish, M., 2013. Dispersion model evaluation of $PM_{2.5}$, NO_x and SO_2 from point and major line sources in Nova Scotia, Canada using AERMOD Gaussian plume air dispersion model. *Atmospheric Pollution Research* 4, 157–167.

Gupta, M., Mohan, M., 2013. Assessment of contribution to PM_{10} concentrations from long range transport of pollutants using WRF/Chem over a subtropical urban airshed. *Atmospheric Pollution Research* 4, 405–410.

Hansard, R., Maher, B.A., Kinnersley, R., 2011. Biomagnetic monitoring of industry–derived particulate pollution. *Environmental Pollution* 159, 1673–1681.

Hao, J.M., Wang, L.T., Shen, M.J., Li, L., Hu, J.N., 2007. Air quality impacts of power plant emissions in Beijing. *Environmental Pollution* 147, 401–408.

Holmes, N.S., Morawska, L., 2006. A review of dispersion modelling and its application to the dispersion of particles: An overview of different dispersion models available. *Atmospheric Environment* 40, 5902–5928.

Hong, S.Y., Noh, Y., Dudhia, J., 2006. A new vertical diffusion package with an explicit treatment of entrainment processes. *Monthly Weather Review* 134, 2318–2341.

Isakov, V., Touma, J.S., Khlystov, A., 2007. A method of assessing air toxics concentrations in urban areas using mobile platform measurements. *Journal of the Air & Waste Management Association* 57, 1286–1295.

Kesarkar, A.P., Dalvi, M., Kaginalkar, A., Ojha, A., 2007. Coupling of the Weather Research and Forecasting Model with AERMOD for pollutant dispersion modeling. A case study for PM_{10} dispersion over Pune, India. *Atmospheric Environment* 41, 1976–1988.

Khamsimak, P., Koonaphapdeelert, S., Tippayawong, N., 2012. Dispersion modeling of SO_2 emissions from a lignite fired thermal power plant using CALPUFF. *Energy and Environment Research* 2, 127–136.

Lee, D.G., Lee, Y.M., Jang, K.W., Yoo, C., Kang, K.H., Lee, J.H., Jung, S.W., Park, J.M., Lee, S.B., Han, J.S., Hong, J.H., Lee, S.J., 2011. Korean national emissions inventory system and 2007 air pollutant emission. *Asian Journal of Atmospheric Environment* 5, 278–291.

Levy, I., Mahrer, Y., Dayan, U., 2009. Coastal and synoptic recirculation affecting air pollutants dispersion: A numerical study. *Atmospheric Environment* 43, 1991–1999.

Liu, N., Yu, Y., He, J.J., Zhao, S.P., 2013. Integrated modeling of urban–scale pollutant transport: Application in a semi–arid urban valley, Northwestern China. *Atmospheric Pollution Research* 4, 306–314.

Lopez, M.T., Zuk, M., Garibay, V., Tzintzun, G., Iniestra, R., Fernandez, A., 2005. Health impacts from power plant emissions in Mexico. *Atmospheric Environment* 39, 1199–1209.

Ma, J., Yi, H., Tang, X., Zhang, Y., Xiang, Y., Pu, L., 2013. Application of AERMOD on near future air quality simulation under the latest national

emission control policy of China: A case study on an industrial city. *Journal of Environmental Sciences* 25, 1608–1617.

Mohan, M., Bhati, S., 2011. Analysis of WRF model performance over subtropical region of Delhi, India. *Advances in Meteorology*, art. no. 621235.

Rama Krishna, T.V.B.P.S., Reddy, M.K., Reddy, R.C., Singh, R.N., 2004. Assimilative capacity and dispersion of pollutants due to industrial sources in Visakhapatnam bowl area. *Atmospheric Environment* 38, 6775–6787.

Scire, J.S., Strimaitis, D.G., Yamartino, R.J., 2000a. A User's Guide for the CALPUFF Dispersion Model, Earth Tech, Inc., Concord, Massachusetts, 521 pages.

Scire, J.S., Robe, F.R., Fernau, M.E., Yamartino, R.J., 2000b. A User's Guide for the CALMET Meteorological Model, Earth Tech, Inc., Concord, Massachusetts, 332 pages.

Song, Y., Zhang, M.S., Cai, X.H., 2006. PM_{10} modeling of Beijing in the winter. *Atmospheric Environment* 40, 4126–4136.

Spak, S.N., Holloway, T., 2009. Seasonality of speciated aerosol transport over the Great lakes region. *Journal of Geophysical Research–Atmospheres* 114, art. no. D08302.

Tartakovsky, D., Broday, D.M., Stern, E., 2013. Evaluation of AERMOD and CALPUFF for predicting ambient concentrations of total suspended particulate matter (TSP) emissions from a quarry in complex terrain. *Environmental Pollution* 179, 138–145.

Villasenor, R., Lopez–Villegas, M.T., Eidels–Dubovoi, S., Quintanar, A., Gallardo, J.C., 2003a. A mesoscale modeling study of wind blown dust on the Mexico City Basin. *Atmospheric Environment* 37, 2451–2462.

Villasenor, R., Magdaleno, M., Quintanar, A., Gallardo, J.C., Lopez, M.T., Jurado, R., Miranda, A., Aguilar, M., Melgarejo, L.A., Palmerin, E., Vallejo, C.J., Barchet, W.R., 2003b. An air quality emission inventory of offshore operations for the exploration and production of petroleum by the Mexican oil industry. *Atmospheric Environment* 37, 3713–3729.

Willmott, C., 1984. *On the evaluation of model performance in physical geography*, (Eds.): Gaile, G., Willmott, C., Spatial statistics and models, Springer Netherlands, pp. 443–460.

Zawar–Reza, P., Kingham, S., Pearce, J., 2005. Evaluation of a year–long dispersion modelling of PM_{10} using the mesoscale model TAPM for Christchurch, New Zealand. *Science of the Total Environment* 349, 249–259.

Zhang, Y., Liu, X.H., Olsen, K.M., Wang, W.X., Do, B.A., Bridgers, G.M., 2010. Responses of future air quality to emission controls over North Carolina, Part II: Analyses of future–year predictions and their policy implications. *Atmospheric Environment* 44, 2767–2779.

Zhou, Y., Levy, J.I., Hammitt, J.K., Evans, J.S., 2003. Estimating population exposure to power plant emissions using CALPUFF: A case study in Beijing, China. *Atmospheric Environment* 37, 815–826.

Zou, B., Wilson, J.G., Zhan, F.B., Zeng, Y.N., Wu, K.J., 2011. Spatial–temporal variations in regional ambient sulfur dioxide concentration and source–contribution analysis: A dispersion modeling approach. *Atmospheric Environment* 45, 4977–4985.